Mode-channel interdependence of the vibrational excitations associated with *K*-shell photoionization of CO_2

Yury S. Krivosenko* and Andrey A. Pavlychev†

V. A. Fock Institute of Physics, St. Petersburg State University, 198504 St. Petersburg, Petrodvorets, Ulianovskaya 3, Russia

(Received 28 November 2013; published 31 March 2014)

It is shown that the direction of the photoelectron recoil momentum transferred to the photoion influences molecular photoionization dynamics, resulting in the appearance of a specific mode–channel interdependence. We disclose the interdependence and the interplay of the core-hole- and photoelectron-induced recoil effects by passing to normal mass-dependent modes in both coordinate and momentum spaces. As an example, the vibrational structure of the $1s^{-1}$ photoelectron line of CO_2 is investigated in detail. The intensity of bending and symmetric and asymmetric stretching vibrational and rotational excitations is found to differ substantially in the $\Sigma \rightarrow \Sigma$ and $\Sigma \rightarrow \Pi$ photoionization channels.

DOI: 10.1103/PhysRevA.89.032517 PACS number(s): 33.20.Tp, 33.20.Rm, 33.70.Ca

I. INTRODUCTION

Photoionization is a versatile tool for probing the rotation-vibration-electronic dynamics of molecules. The emitted photoelectrons carry information about the quantum state of the residual molecular ion. In this work the relationship between the molecular final quantum state and hard-x-ray inner-shell photoionization dynamics is investigated and discussed.

In the near-edge regime the relationship is governed by the Franck-Condon principle: nuclear positions and momenta in the molecular frame can be reasonably accounted as unchanged during the ionization process [1,2]. In this case vibrational excitations associated with inner-shell ionization are caused by the core-hole effect. Their distribution obeys the Franck-Condon relation. The exceptions are mainly due to strong intramolecular interference of the photoelectron waves [3,4]. Another situation is realized far from the x-ray absorption edge, where the interference plays a minor role. In addition to the core-hole effect the high-kinetic-energy photoelectron gains momentum, which results in complicated photoionization dynamics [5]. The vibrational transitions demonstrate substantial non-Franck–Condon behavior as the nuclear momenta can no longer be regarded as unchanged. Thus, the molecular final quantum state becomes substantially dependent on the magnitude and orientation of the transferred momentum relative to the molecular frame.

Domcke and Cederbaum were the first to predict and describe the recoil effect attending a molecular photoionization in diatomic molecules [5]. During the last decade the photoelectron-induced recoil effect was studied in detail both experimentally and theoretically [6–11]. Molecular rotational recoil during valence photoionization of N_2 and CO was investigated [6,7], and translational recoil was detected in Auger decay following Ar $1s$ photoionization [8]. Sun *et al.* [9] examined the rotational Doppler effect in the photoelectron spectra of free molecules. The focus of the investigations is to study the dependence of recoil effects on the magnitude of the transferred momentum. Regrettably, the orientational dependence was not examined, whereas the observed increase of asymmetric vibrational excitations in C $1s$ photoionization of CH_4 [10] and CF_4 [11] indicates its significance. The dependence has attracted our attention, and we consider it using the example of CO_2. Substantial mode-channel interdependence of the C and O $1s^{-1}$ photoelectron lines is predicted and described in detail.

II. MODE-CHANNEL INTERDEPENDENCE

A. General relations

To study the connection between the transferred recoil momentum and vibrational excitations the Born-Oppenheimer approximation is applied. In this framework the photoionization amplitude is a product of electronic core-to-continuum ($A_{\rm el}$) and nuclear-subsystem ($A_{\rm nuc}$) transition amplitudes [12]. Assuming that the rovibrational coupling is neglected, $A_{\rm nuc}$ is a product of vibrational and rotational transition amplitudes. The amplitudes generate the distribution functions $f_{v'}$ and $f_{N'}$ and thereby the mean vibrational and rotational energies in the final state. In order to obtain the amplitudes we decompose the nuclear-subsystem motion over the normal modes, we use the momentum representation [5,10] and apply the dynamic core-hole localization [13,14] approach.

The normal mass-dependent coordinates R are linked with the Cartesian displacements r from the equilibrium positions as [2,15]

$$r = M^{-1/2} T\, \mathsf{R} = \mathcal{A}\, \mathsf{R}. \tag{1}$$

Here r and R are the N-dimensional vectors ($N = 3n$, where n is the number of nuclei in the molecule), $M = \mathrm{diag}\,(m_1, m_2, \ldots, m_{3n})$, $m_{3k-2} = m_{3k-1} = m_{3k}$ is the k-*th* atom mass. The T matrix diagonalizes the matrix $V = M^{-1/2} U M^{-1/2}$, where the elements of U are defined as potential function second derivatives over the atomic displacements r. The diagonal matrix $T^{\mathsf{T}} V T = \mathrm{diag}\,(\omega_1^2, \omega_2^2, \ldots, \omega_N^2)$ is composed of the squares of the normal vibration frequencies. Even in the case of ω zero eigenvalues or degeneracy the T matrix can be reduced to the unitary form, which is used hereafter. The property $T^{-1} = T^{\dagger} = T^{\mathsf{T}}$ for the real T matrix is utilized afterwards.

*y.krivosenko@gmail.com
†andrey.pavlychev@gmail.com

The linkage between the ordinary momenta p and normal mass-dependent momenta P is

$$p = M^{1/2}\,T\,\mathsf{P} = \mathcal{B}\,\mathsf{P}, \quad \mathsf{P} = T^{\mathsf{T}}\,M^{-1/2}p = \mathcal{B}^{-1}\,p. \tag{2}$$

Since the T matrices in the r and p spaces diagonalize the same V matrix, they can be designed to be identical:

$$\mathcal{A}^{-1} = \mathcal{B}^{\mathsf{T}} \quad \text{and} \quad \mathcal{B}^{-1} = \mathcal{A}^{\mathsf{T}}.$$

Thus, no separate computations of the normal modes in r and p spaces are required.

Presenting the Hamiltonian in normal momenta as

$$\widehat{H}_p = \sum_i \left[\frac{1}{2}\mathsf{P}_i^2 - \frac{\hbar^2}{2}\omega_i^2\frac{\partial^2}{\partial \mathsf{P}_i^2}\right], \tag{3}$$

we express the mean recoil energy as a sum over degrees of freedom i (or independent molecular motion modes):

$$\Delta E_i = \tfrac{1}{2}(\Delta \mathsf{P}_i)^2 = \tfrac{1}{2}(\{\mathcal{B}^{-1}\,\Delta p\}_i)^2. \tag{4}$$

To construct the N-vector Δp the dynamic core-hole localization approximation [13,14] is used and photoelectron recoil momentum is considered to be transferred to the core-ionized atom (the kth atom). In the laboratory frame the recoil momentum $\Delta\vec{p}$ is opposite to the primary photoelectron momentum $\vec{p}_e$: $\Delta\vec{p} = -\vec{p}_e$. The recoil leads to translation of the molecule's center of mass and internal vibrational and rotational excitations. Considering photoelectron ejection along the single Cartesian direction (j), we present $\Delta p_{j'} = -p_e\,\delta_{jj'}$, where $\delta_{jj'}$ is the Kronecker delta. Therefore

$$\Delta \mathsf{P}_i(j) = \mathcal{B}^{-1}\Delta p = -p_e(\mathcal{B}^{-1})_{ij}. \tag{5}$$

Then the mean recoil energy ΔE_{ij} associated with the ith motion mode and the jth ejection direction is

$$\Delta E_{ij} = \tfrac{1}{2}[\Delta \mathsf{P}_i(j)]^2 = K_e m_e\,\mathcal{C}_{ij}. \tag{6}$$

Equation (6) demonstrates linear dependence of ΔE_{ij} on the photoelectron kinetic energy K_e with the corresponding slope determined by the matrix element $\mathcal{C}_{ij} = [(\mathcal{B}^{-1})_{ij}]^2$. Also Eq. (6) determines the mode-channel (i-j) interdependence. The interdependence is valid for the high-kinetic-energy regime in which the transferred momentum is opposite to the photoemission direction. In the general case the simple relationship between the directions is broken due to intramolecular interference of the primary and scattered photoelectron waves.

B. Application to CO_2

To study the mode-channel interdependence C and O K-shell ionization of CO_2 is investigated. In the ground state the molecule possesses $D_{\infty h}$ point-group symmetry and its molecular dynamics includes bending and asymmetric and symmetric stretching vibrational, translational, and rotational motion. Taking into account that far from the $1s$ ionization thresholds the photoelectron angular distributions corresponding to $\Sigma \to \Sigma$ and $\Sigma \to \Pi$ photoionization channels approach the atomic limits, we identify the channels with $1s \to p_z$ and $p_{x,y}$ transitions [16], respectively. It is supposed here that z is parallel to the molecular axis. Hence, the direction $\vec{p}_e$ specifies participation of the j channel in the photoionization event. Near the thresholds this specification is not possible as the photoelectron angular distributions in CO_2 are strongly dependent on K_e and do not coincide with the atomic ones [17].

The T matrix results from solving the corresponding secular equation; then the matrices $\mathcal{A}$, $\mathcal{B}$, and $\mathcal{C}$ are determined. The transposed $\mathcal{C}$ matrix is presented below:

$$\mathcal{C}^{\mathsf{T}} = \left(\begin{array}{cccccc|l}
\frac{1}{2M} & 0 & \frac{m}{2M\mathcal{M}} & 0 & \frac{1}{\mathcal{M}} & 0 & (j=1)\,\mathrm{O_{left}}\ 1s\ \Sigma\to\Sigma \\
0 & \frac{m}{2M\mathcal{M}} & 0 & \frac{1}{2M} & 0 & \frac{1}{\mathcal{M}} & (j=2)\,\mathrm{O_{left}}\ 1s\ \Sigma\to\Pi \\
0 & 0 & \frac{2M}{m\mathcal{M}} & 0 & \frac{1}{\mathcal{M}} & 0 & (j=3)\,\mathrm{C}\ 1s\ \Sigma\to\Sigma \\
0 & \frac{2M}{m\mathcal{M}} & 0 & 0 & 0 & \frac{1}{\mathcal{M}} & (j=4)\,\mathrm{C}\ 1s\ \Sigma\to\Pi \\
\frac{1}{2M} & 0 & \frac{m}{2M\mathcal{M}} & 0 & \frac{1}{\mathcal{M}} & 0 & (j=5)\,\mathrm{O_{right}}\ 1s\ \Sigma\to\Sigma \\
0 & \frac{m}{2M\mathcal{M}} & 0 & \frac{1}{2M} & 0 & \frac{1}{\mathcal{M}} & (j=6)\,\mathrm{O_{right}}\ 1s\ \Sigma\to\Pi \\
\hline
\uparrow & \uparrow & \uparrow & \uparrow & \uparrow & \uparrow & \uparrow \\
i=1 & i=2 & i=3 & i=4 & i=5 & i=6 & \text{photoionization channel}
\end{array}\right). \tag{7}$$

Here M, m, and $\mathcal{M}$ are the oxygen and carbon atomic masses and the total molecular mass, respectively. The column numbers $i = 1,2,\ldots,6$ label the symmetric stretching, bending, and asymmetric stretching vibration modes, molecular rotation, and translations along and perpendicular to the molecular axis, respectively. The row numbers $j = 1,2,\ldots,6$ label the photoionization channels. Bending vibrations and rotations as well as C and O $1s\ \Sigma\to\Pi$ transitions are doubly degenerate. This explains the reduction of the $\mathcal{C}$ matrix dimension. We point out that the results are directly applicable to K-shell photoionization of the CS_2 molecule.

Using (6) and (7) the analysis of the mean recoil energy ΔE_{ij} is performed. In contrast to the translational recoil, independent of the photoionization channels, the internal molecular excitations demonstrate strong mode-channel interdependence. Specifically, the O $1s\ \Sigma\to\Pi$ channel is accompanied by rotational and bending excitations, the O $1s\ \Sigma\to\Sigma$ channel is accompanied by symmetric and asymmetric stretching excitations, and the C $1s\ \Sigma\to\Sigma$ and Π channels are associated with asymmetric stretching and bending excitations, respectively. For example, the relation $\Delta E_{11} = \Delta E_{15} = \Delta E_{42} = \Delta E_{46}$ means equal shifts of the

binding energy due to the photoelectron-induced rotations in O $1s\ \Sigma \rightarrow \Pi$ and symmetric stretching vibrations in the O $1s\ \Sigma \rightarrow \Sigma$ channel.

Both rotational and vibrational excitations lead to increase of the population of high N' and v' levels in the ionic state in comparison with the population in the ground state. Since individual N' levels are not resolved in inner-shell and valence photoelectron spectra [6], the distribution of rotational excitations is left aside. But changes in the vibrational structures of the C and O $1s^{-1}$ photoelectron lines attract our main attention below.

III. INTERPLAY OF CORE-HOLE AND PHOTOELECTRON RECOIL EFFECTS

A. General relations

The amplitudes of vibrational transitions associated separately with the core-hole and recoil effects are

$$\langle v_i'|0\rangle_r = \int \chi^*_{v_i'}(\mathsf{R}_i + \Delta\mathsf{R}_i)\chi_0(\mathsf{R}_i)d\mathsf{R}_i \tag{8}$$

and

$$\langle v_i'|0\rangle_p = \int \chi^*_{v_i'}(\mathsf{P}_i + \Delta\mathsf{P}_i)\chi_0(\mathsf{P}_i)d\mathsf{P}_i, \tag{9}$$

where $\Delta\mathsf{R}_i$ is the shift of the equilibrium position along the ith mode and $\Delta\mathsf{P}_i$ is the total photoelectron recoil momentum transferred to the ith mode. The functions χ_0 and $\chi_{v_i'}$ describe molecular vibrations in the ground and ionized states. The subscripts r and p indicate the coordinate and momentum spaces, respectively. It is supposed that zero-point molecular vibrations dominate in the ground state.

To combine the core-hole and photoelectron-recoil effects on the intensity of vibrational transitions we at first present $\Delta\mathsf{R}_i$ and $\Delta\mathsf{P}_i$ in terms of integral operators $\Delta\widehat{\mathsf{R}}_i$ and $\Delta\widehat{\mathsf{P}}_i$ shifting the variables of $|0\rangle$ relative to $|v_i'\rangle$:

$$\begin{aligned} c\langle v'|0\rangle_r &= \langle v_i'|\Delta\widehat{\mathsf{R}}_i|0\rangle \\ &= \iint \chi^*_{v_i'}(\mathsf{R}_i')\delta(\mathsf{R}_i' - (\mathsf{R}_i + \Delta\mathsf{R}_i))\ \chi_0(\mathsf{R}_i)\, d\mathsf{R}_i' d\mathsf{R}_i \end{aligned} \tag{10}$$

and

$$\begin{aligned} \langle v_i'|0\rangle_p &= \langle v_i'|\Delta\widehat{\mathsf{P}}_i|0\rangle \\ &= \iint \chi^*_{v_i'}(\mathsf{P}_i')\delta(\mathsf{P}_i' - (\mathsf{P}_i + \Delta\mathsf{P}_i))\ \chi_0(\mathsf{P}_i)\, d\mathsf{P}_i' d\mathsf{P}_i, \end{aligned} \tag{11}$$

where $\delta(x)$ is the Dirac delta function. Then the combined vibrational transition amplitudes are presented as

$$A_{0\rightarrow v_i'} = \langle v_i'|\ \Delta\widehat{\mathsf{P}}_i\ \Delta\widehat{\mathsf{R}}_i\ |0\rangle \tag{12}$$

or

$$A_{0\rightarrow v_i'} = \langle v_i'|\ \Delta\widehat{\mathsf{R}}_i\ \Delta\widehat{\mathsf{P}}_i\ |0\rangle. \tag{13}$$

Integrating (12) gives

$$\begin{aligned} A_{0\rightarrow v_i'} = \langle v_i'|\Delta\widehat{\mathsf{P}}_i\Delta\widehat{\mathsf{R}}_i|0\rangle = \iiiint d\mathsf{P}d\mathsf{P}'d\mathsf{R}d\mathsf{R}' \\ \times\langle v_i'|\mathsf{P}'\rangle\ \langle\mathsf{P}'|\Delta\widehat{\mathsf{P}}_i|\mathsf{P}\rangle\langle\mathsf{P}|\mathsf{R}'\rangle\langle\mathsf{R}'|\Delta\widehat{\mathsf{R}}_i|\mathsf{R}\rangle\langle\mathsf{R}|0\rangle. \end{aligned}$$

Integrating (13) gives a similar result. Here $\langle\mathsf{P}|\mathsf{R}'\rangle \propto \exp(-i\mathsf{P}\mathsf{R}'/\hbar)$.

Then, neglecting the difference in vibrational quanta in the ground and ionic states we reduce the total distribution of vibrational excitations to a Poisson distribution:

$$f_{0\rightarrow v_i'} = \mathrm{Pois}_{v_i'}\left(\frac{\omega_i(\Delta\mathsf{R}_i)^2}{2\,\hbar} + \frac{(\Delta\mathsf{P}_i)^2}{2\,\hbar\omega_i}\right). \tag{14}$$

Equation (14) shows that the expectation value a_i of the $0 \rightarrow v_i'$ excitation is a sum of the expectations corresponding to the core-hole creation [$a_{\mathrm{core},i} = \omega_i(\Delta\mathsf{R}_i)^2/2\hbar$] and photoelectron-induced recoil [$a_{\mathrm{rec},i} = (\Delta\mathsf{P}_i)^2/2\hbar\omega_i$] effects.

Considering photoionization in the j-th channel, the expectation value of the $0 \rightarrow v_i'$ transition is

$$a_{ij} = \frac{\omega_i(\Delta\mathsf{R}_i)^2}{2\hbar} + \frac{K_e m_e\, \mathcal{C}_{ij}}{\hbar\omega_i}. \tag{15}$$

Equations (14) and (15) make evident the mode-channel interdependence of the vibrational excitations. The matrix element a_{ij} is dependent on the dynamic core-hole localization, the photoelectron kinetic energy, and the direction of the photoelectron transferred momentum. Since both terms in the right-hand side of (15) are positive, the intensity of vibrational excitations increases due to the common action of the core-hole and photoelectron-induced recoil.

B. Application to CO_2 and discussion

To illustrate the interplay of the core-hole and the photoelectron recoil effects (Sec. III A) and the mode–channel interdependence (Sec. II) K-shell photoemission from both fixed-in-space and randomly oriented CO_2 is examined. The vibrational structure of the C and O $1s^{-1}$ photoelectron lines for parallel ($\Sigma \rightarrow \Sigma$) and perpendicular ($\Sigma \rightarrow \Pi$) transitions for kinetic energies 100 eV, 1 keV and 8 keV, is computed using (14). The calculated spectra of the fixed-in-space molecule are plotted in Figs. 1(a) and 1(b). The spectra averaged over all molecular orientations are shown in Fig. 1(c). The vibration structure corresponding to the lowest K_e (solid line in Fig. 1) is regarded as a reference to demonstrate the vibrational excitations associated with the core-hole effect, as the recoil effect plays a minor role in their formation. The calculations are performed using the empirical values $a_{\mathrm{core},1}(\mathrm{C}\ 1s) \simeq 0.262$, $a_{\mathrm{core},2}(\mathrm{C}\ 1s) = a_{\mathrm{core},3}(\mathrm{C}\ 1s) \approx 0$, $a_{\mathrm{core},3}(\mathrm{O}\ 1s) \simeq 0.553$, and $a_{\mathrm{core},1}(\mathrm{O}\ 1s) = a_{\mathrm{core},2}(\mathrm{O}\ 1s) \approx 0$ taken from the experimental inner-shell photoemission spectra of CO_2 [18–22]. The parameters serve to specify the core-hole effect on the vibrational transitions. In Fig. 1 each structure is the overlap of Lorentzian-shaped individual vibrational transitions with the full width at half maximum of approximately 0.165 eV [20] and 0.097 eV [19] corresponding to the O and C $1s$ hole lifetimes and the vibrational quanta $\hbar\omega_1 = 0.165$ eV [19], $\hbar\omega_2 = 0.083$ eV [23], and $\hbar\omega_3 = 0.307$ eV [21]. In Figs. 1(b) and 1(c) rotational recoil-induced excitations in O $1s$ spectra are taken into account by the shifts $\Delta E_{42(46)}$ and $2/3\,\Delta E_{42(46)}$, respectively. Translational recoil is also included by the corresponding spectral shift; see (6) and (7). The calculations are performed using SAGE mathematics software [24].

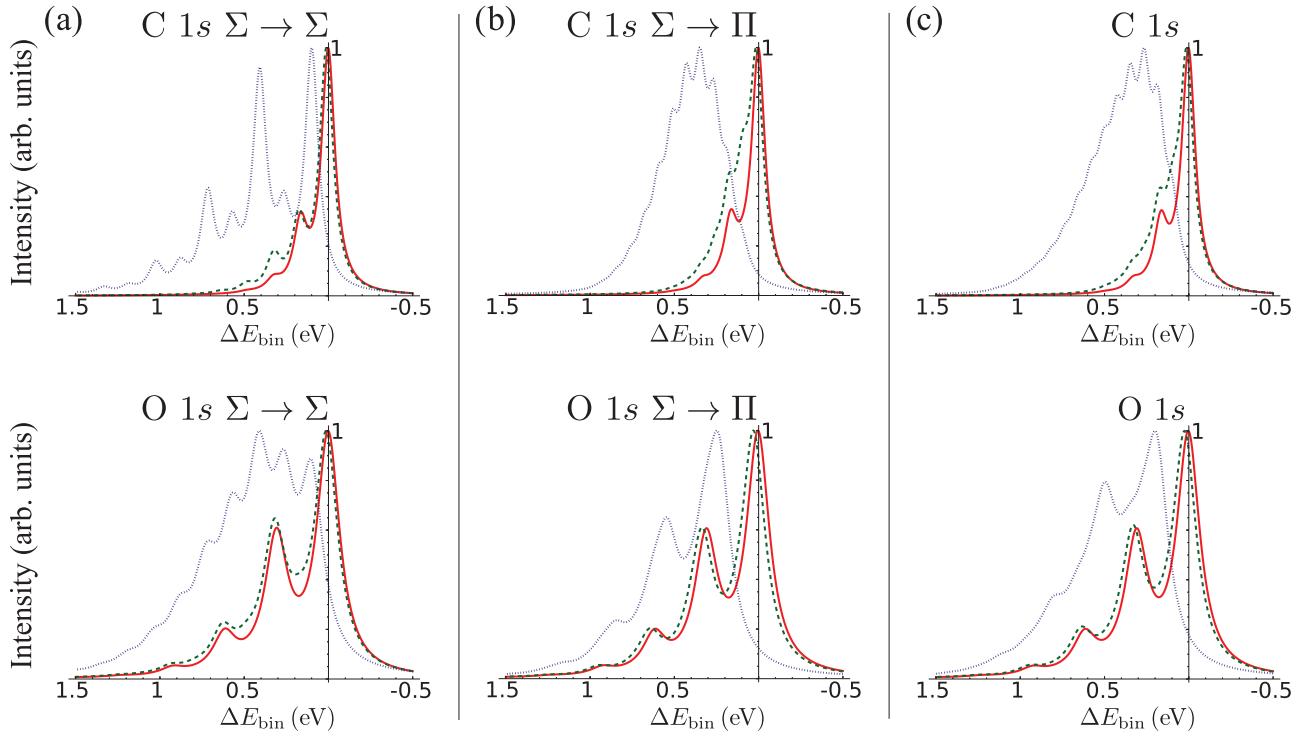

FIG. 1. (Color online) C 1s and O 1s photoelectron lines of CO_2 for (a) $\Sigma \rightarrow \Sigma$, (b) $\Sigma \rightarrow \Pi$, and (c) for a randomly oriented molecule. The photoelectron kinetic energies are 100 eV (solid line), 1 keV (dashed line), and 8 keV (dotted line). The spectra are normalized to the maximum.

The computed structures in Fig. 1 show strong mode-channel interdependence. There are perceptible changes in the vibrational structure due to the photoelectron-induced recoil at $K_e = 1$ keV and huge changes at $K_e = 8$ keV. Analyzing them we see the different shifts ΔE_{ij} of the photoelectron line centroid originating from molecular rotations and the relevant vibrational excitations. In addition to the shifts one may see strong changes in the relative intensity of vibrational excitations. The vibrational structures corresponding to the $\Sigma \rightarrow \Sigma$ and $\Sigma \rightarrow \Pi$ transitions become substantially different. In particular, bending vibrations dominate in the C 1s $\Sigma \rightarrow \Pi$ channel, whereas asymmetric stretching vibrations do in the C 1s $\Sigma \rightarrow \Sigma$ channel. Both bending and rotational excitations dominate in the O 1s $\Sigma \rightarrow \Pi$ channel, but symmetric vibrations become predominant in the O 1s $\Sigma \rightarrow \Sigma$ channel. Such vibrational modes as asymmetric stretching and bending in C 1s photoionization, as well as symmetric stretching and bending in O 1s photoionization, suppressed in the low-kinetic-energy regime, are considerably enhanced at high K_e.

The revealed mode-channel interdependence is a general phenomenon in molecular photoeffects. This is supported by the C 1s photoelectron spectra of CF_4 measured at photon energies from 330 to 1500 eV [11]. These spectra evidence that the contribution of asymmetric vibrational modes to the C $1s^{-1}$ line increases linearly as the photoelectron kinetic energy increases [11], demonstrating close resemblance to the increase of asymmetric vibrations of CO_2. In both spectra the asymmetric vibrations are strongly suppressed at low kinetic energies. Using (6) and (7), we present the mean recoil energy referring to excitation of both asymmetric modes in CF_4 as $K_e m_e 4M_F/m(m + 4M_F)$ and obtain approximately 39.3 meV for emission of C 1s photoelectrons with $K_e = 1$ keV. The recoil energy is in good agreement with the numerical calculation performed with the Hartree-Fock, Becke three-parameter Lee-Yang-Parr, and coupled-cluster theory with single, double, and partially triple excitations methods in [11]. We also predict [see (14) and (15)] nearly linear energy dependence of the intensity ratio $f_{v=1}/f_{v=0}$ for the recoil-induced asymmetric mode. As to the nonlinear dependence of the ratio, which the authors of [11] extracted from the decomposition of the experimental spectra, it demands a more detailed analysis. We have looked at the dependence, but regrettably the narrowness of the spectral interval in Fig. 1 in [11] does not allow performing a full-scale study.

IV. CONCLUSION

In conclusion we note that the direction of the transferred photoelectron momentum substantially influences the quantum state of the remaining molecular ion. In the high-kinetic-energy regime the photoelectron line becomes dependent on the photoionization channel, demonstrating the mode-channel interdependence that links the distribution of vibrational excitations with the magnitude and direction of the photoelectron momentum transferred to a core-ionized atom. In contrast to the σ^* shape resonance, for which the distributions of vibrational excitation are also different in the $\Sigma \rightarrow \Sigma$ and $\Sigma \rightarrow \Pi$ channels, the mode dependence cannot be rationalized in the framework of the Franck-Condon principle.

Further investigations of the mode-channel interdependence including anharmonicity of photoelectron-induced vibrations and rovibrational coupling are of significance. They

open additional perspectives in determination of the spectroscopic parameters of free, aligned, and encapsulated core-excited molecules. Using the mode-channel interdependence the equilibrium interatomic distances in core-excited linear triatomic (such as N_2O and OCS) and more complex molecular species could be directly measured without any preliminary calculations. Recently the quasimolecular recoil (QMR) model has been suggested to describe the characteristic spectral changes of the $1s^{-1}$ photoelectron line induced by the photoion recoil and to link the changes with chemical bonds between adsorbate and substrate atoms [25]. Further investigations of the mode-channel interdependence in the framework of the QMR model open further perspectives for surface studies.

ACKNOWLEDGMENT

The work is supported by the RFBR Grants No. 12-02-00999 and No. 12-02-31415 and SPbU Grant No. 11.38.638.2013.

[1] P. W. Atkins and R. S. Friedman, *Molecular Quantum Mechanics* (Oxford University Press, Oxford, 1999).
[2] L. A. Gribov, V. I. Baranov, and D. Yu. Zelentsov, *Electronic-Vibrational Spectra of Polyatomic Molecules: Theory and Methods of Calculation* (Nauka, Moscow, 1997).
[3] J. L. Dehmer, D. Dill, and A. C. Parr, in *Photophysics and Photochemistry in the Vacuum Ultraviolet*, edited by S. McGlynn, G. Findly, and R. Huebner (Reidel, Dordrecht, 1985), p. 341.
[4] A. A. Pavlychev and D. A. Mistrov, J. Phys. B **42**, 055103 (2009).
[5] W. Domcke and L. S. Cederbaum, J. Electron Spectrosc. Relat. Phenom. **13**, 161 (1978).
[6] T. D. Thomas *et al.*, Phys. Rev. A **79**, 022506 (2009).
[7] E. Kukk, T. D. Thomas, and K. Ueda, J. Electron Spectrosc. Relat. Phenom. **183**, 53 (2011).
[8] R. Guillemin, C. Bomme, T. Marin, L. Journel, T. Marchenko, R. K. Kushawaha, N. Trcera, M. N. Piancastelli, and M. Simon, Phys. Rev. A **84**, 063425 (2011).
[9] Y.-P. Sun, Ch.-K. Wang, and F. Gel'mukhanov, Phys. Rev. A **82**, 052506 (2010).
[10] E. Kukk *et al.*, Phys. Rev. Lett. **95**, 133001 (2005).
[11] T. D. Thomas *et al.*, J. Chem. Phys. **128**, 144311 (2008).
[12] A. S. Davydov, *Quantum Mechanics* (Nauka, Moscow, 1973).
[13] A. A. Pavlychev, N. G. Fominykh, N. Watanabe, K. Soejima, E. Shigemasa, and A. Yagishita, Phys. Rev. Lett. **81**, 3623 (1998).
[14] E. S. Klyushina *et al.*, Contemp. Math. Fundamental Direc. **48**, 61 (2013).
[15] U. Hergenhahn, J. Phys. B **37**, R89 (2004).
[16] A. De Fanis *et al.*, Phys. Rev. Lett. **89**, 023006 (2002).
[17] N. Watanabe, J. Adachi, K. Soejima, E. Shigemasa, A. Yagishita, N. G. Fominykh, and A. A. Pavlychev, Phys. Rev. Lett. **78**, 4910 (1997).
[18] M. Schmidbauer, A. L. D. Kilcoyne, H.-M. Köppe, J. Feldhaus, and A. M. Bradshaw, Phys. Rev. A **52**, 2095 (1995).
[19] T. X. Carroll, J. Hahne, T. D. Thomas, L. J. Saethre, N. Berrah, J. Bozek, and E. Kukk, Phys. Rev. A **61**, 042503 (2000).
[20] K. Maier, A. Kivimäki, B. Kempgens, U. Hergenhahn, M. Neeb, A. Rüdel, M. N. Piancastelli, and A. M. Bradshaw, Phys. Rev. A **58**, 3654 (1998).
[21] M. Hoshino *et al.*, J. Phys. B **39**, 3655 (2006).
[22] M. Kimura, M. Takekawa, Y. Itikawa, H. Takaki, and O. Sueoka, Phys. Rev. Lett. **80**, 3936 (1998).
[23] A. Kivimäki, B. Kempgens, K. Maier, H. M. Köppe, M. N. Piancastelli, M. Neeb, and A. M. Bradshaw, Phys. Rev. Lett. **79**, 998 (1997).
[24] W. A. Stein *et al.*, programming language SAGE, Version 5.7 (Sage Development Team, 2013), http://www.sagemath.org
[25] Yu. S. Krivosenko and A. A. Pavlychev, Chem. Phys. Lett. **575**, 107 (2013).